Congresso de Métodos Numéricos em Engenharia 2015
Lisboa, 29 de Junho a 2 de Julho, 2015

EVALUATION OF A NEW PHENOMENOLOGICAL CYCLIC ELASTIC-PLASTIC APPROACH FOR MAGNESIUM ALLOYS

Vitor Anes, Manuel Freitas and Luis Reis

IDMEC, Instituto Superior Técnico, Universidade de Lisboa
Av. Rovisco Pais, 1049-001 Lisboa, Portugal.
e-mail: luis.g.reis@ist.utl.pt

Keywords: Cyclic plasticity, simulation, magnesium alloys, LCF, AZ31B-F.

Abstract *Magnesium alloys are greatly appreciated due to their high strength to weight ratio, stiffness, and low density. However, Mg alloys can exhibit complex types of cyclic plasticity like twinning, de-twinning or Bauschinger effect. Recent studies indicate that these type of cyclic plastic deformations cannot be fully characterized using the typical tools usually used in the cyclic characterization of steels, thus it is required new approaches to fully capture their cyclic deformation and plasticity. This study aims to evaluate a phenomenological cyclic elastic-plastic approach implemented to capture the cyclic deformation of magnesium alloys under multiaxial loading conditions. In this evaluation, it is performed a correlation between the estimates of the phenomenological approach and the Jiang & Sehitoglu model, a well-established elastic-plastic model easily found in literature. Moreover, these estimates are also correlated with the cyclic elastic-plastic experimental data. Results show good correlations between experiments and the estimates of the phenomenological approach. Some remarks regarding the phenomenological approach and the state-of-the–art elastic-plastic model are drawn.*

1. INTRODUCTION

Cyclic plasticity is quite different from the one obtained under static loading conditions. Under cyclic loadings, materials tend to vary their mechanical properties according to their microstructure and loading regimens, due to that, stress states considered in design stages can be different from the ones experienced in the field, thus it is important entering with the material cyclic elastic-plastic behaviour in mechanical design stages improving results [1]. In the field, components and structures are usually subjected to cyclic multiaxial loadings, which may have constant or variable amplitude with different deformation mechanisms [2]. Under multiaxial loading regimes, the stress-strain response is very different from the uniaxial monotonic curve [3, 4]. However, elastic-plastic models embedded in commercial finite element packages are setup with monotonic stress-strain curves, which are unsuitable to simulate cyclic plasticity. Moreover, the monotonic stress-strain curve is a specific loading case among many others that have different stress-strain relations. In order to modulate quasi-static multiaxial plasticity behaviour, plasticity models have mainly three functions to estimate stress-strain relations for any kind of loading type. These functions are the yield function, hardening rule, and the flow rule, which are setup based in the quasi-static response of a material under uniaxial loading conditions. However, under cyclic loading conditions, the conventional plasticity models have some limitations to capture the cyclic elastic-plastic behaviour because they are strongly dependent on the stress tensor invariants, which in their conventional definition do not have mechanisms to capture complex anisotropies such the ones found in magnesium alloys. Therefore, materials with non-standard cyclic behaviour are not well modulated with this type of models.

Albinmusa et al. [2, 5–7] stated that it is need cyclic anisotropic plasticity models to cover the cyclic behaviour of magnesium alloys, under this statement a question may be raised: will be possible characterize the material anisotropy based only in one loading reference as found in constitutive models? From experiments it was found that magnesium allows have a nonlinear cyclic behaviour, which is dependent of many factors such as strain rate and microstructure deformation mechanisms [1].

Thus, instead of using one uniaxial stress-strain curve obtained under quasi-static loading conditions, why not to use several cyclic and biaxial stress-strain curves to map the material anisotropy in order to update the stress-strain cyclic relation according to the loading type and load level? This type of approach is only possible using phenomenological procedures in which the material cyclic behaviour can be fairly well modulated. There are very few works in literature regarding multiaxial stress-strain relations for magnesium alloys [6, 8–12], but all of them stated that the magnesium alloys cyclic behaviour is quite different from the one found in steels or even in aluminium alloys. One evidence of this difference is the hysteresis loop asymmetry found in magnesium alloys, where the yield stress at compression is quite different from the one in tension; also the rate variation of these values is also different [13,14].

Commercial finite element packages do not have mechanisms to deal with this asymmetry. They assume that the stress in tension and compression are equal in absolute value for the same strain amplitude (which can be accepted true for steels), this means that the plastic strain estimates in tension and compression are considered equal, which is not true for magnesium alloys [2, 8]. Moreover, back stresses in tension and compression do not have equal absolute values in magnesium alloys [14]. The problem complexity increases when it is considered multiaxial loading conditions, where yield stresses, hardening and flow rules vary in a different ways accordingly to the loading type and load level [15,16].

Thus, how it is possible to define a yield function that usually is based in the equivalent stress concept to capture this anisotropy? This work presents a new phenomenological approach that estimates the cyclic elastic-plastic behaviour of magnesium alloys. This approach is based in a stress-strain mapping of the AZ31B-F magnesium alloy subjected to a wide range of cyclic strains under uniaxial and multiaxial loading conditions.

At the present state of the art, it is not possible to accurately estimate the stress-strain relation of magnesium alloys using the available constitutive plasticity models, especially under multiaxial loading conditions. In order to validate the phenomenological approach, the numeric estimates were correlated with experimental data and with the estimates of the well-known Jiang & Sehitoglu plasticity model. Results show that the majority of the phenomenological estimates are in agreement with the experimental data. Some differences between the Jiang & Sehitoglu model and the implemented phenomenological approach are pointed out.

2. THEORETICAL DEVELOPMENTS

2.1 Jiang &Sehitoglu plasticity model

The Jiang & Sehitoglu plasticity model is a non-linear kinematic hardening model that incorporates an Armstrong-Frederick type-hardening rule, in order to capture the Bauschinger effect during a cyclic elastic-plastic deformation [9,17]. It was firstly implemented with the purpose of modulating the cyclic ratcheting phenomena, which is a progressive and directional plastic deformation when a material is subjected to asymmetric loadings under stress control loading regimens [12,17,18], this feature makes this model a good candidate to estimate the elastic-plastic behaviour of magnesium alloys. One peculiarity in this model is the use of a non-proportional hardening parameter to account with the additional resistance of plastic deformations under non-proportional loadings [9]. Moreover, it has a memory function to describe the strain range dependency of the cyclic hardening during the material behaviour simulation. The key equations are presented in Eq. (s) (1) to (4). The yield function, F, is defined as follows:

$$F = \left(\tilde{S} - \tilde{\alpha}\right) : \left(\tilde{S} - \tilde{\alpha}\right) - 2k^2 = 0 \tag{1}$$

Where $\tilde{S}$ is the deviatoric stress tensor, $\tilde{\alpha}$ is the back stress and k is the yield stress. The flow rule is given in Eq. (2).

$$d\tilde{\varepsilon}^p = H \left\langle d\tilde{S} : \tilde{n} \right\rangle \tilde{n} \tag{2}$$

Where $\tilde{\varepsilon}^p$ is the exterior normal unit. The hardening rule is presented in Eq. (3)

$$\tilde{\alpha} = \sum_{i=1}^{M} \tilde{\alpha}^i \tag{3}$$

Material memory contained in the back stress terms is given by the plastic modulus function presented in Eq. (4).

$$H = \sum_{i=1}^{M} c^i r^i \left[1 - \frac{\left|\tilde{\alpha}^i\right|^{X^{i+1}}}{r^i} \tilde{L}^i : \tilde{n} \right] + \sqrt{2}\frac{dk}{dp} \tag{4}$$

2.2 Phenomenological elastic-plastic modulation

From experiments, it was found that the AZ31 magnesium alloy hysteresis loops can be approximated with very acceptable results using a third degree polynomial functions for any value of total-strain. In order to obtain these functions, it is considered six specific points on a hysteresis loop, please see Figure 1. For the left hysteresis branch, the polynomial function is obtained by interpolation using the experimental data obtained at points 4, 5, 6 and 1.

Similarly, the polynomial function of the hysteresis branch at right is obtained using the experimental data of points 4, 3, 2 and 1. The experimental data of these points (1 to 6) vary accordingly to the total strain and strain amplitude ratio $\lambda = \gamma/\varepsilon$. With these polynomials it is possible to capture the magnesium cyclic plastic mechanisms such as twinning, de-twinning, and slip effects at each total strain level and strain amplitude ratios. Where the functions $P_1(\varepsilon_{hs},\lambda)$ and $P_4(\varepsilon_{hs},\lambda)$ estimate two yield stresses regarding the right and left side of the hysteresis loop for the maximum total strain. The functions $P_2(\varepsilon_{hs},\lambda)$ and $P_5(\varepsilon_{hs},\lambda)$ estimate the plastic strains inherent to the maximum total strain, and the functions $P_3(\varepsilon_{hs},\lambda)$ and $P_6(\varepsilon_{hs},\lambda)$ estimate the back stresses.

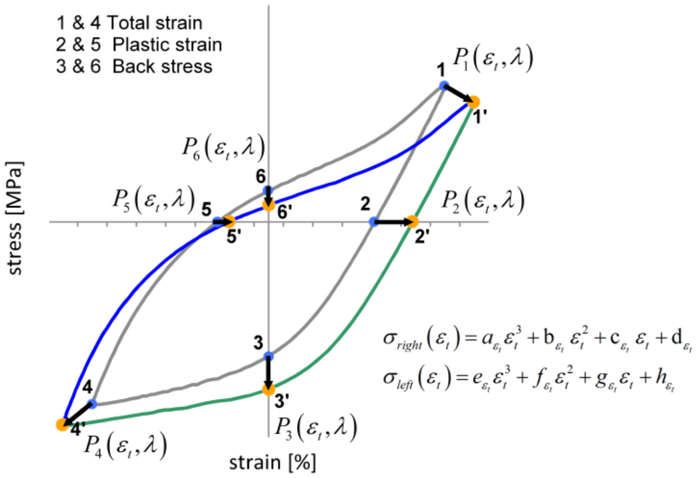

Figure 1. Magnesium alloy hysteresis loop obtained from the axial component of a biaxial loading.

Under biaxial loading conditions, it is obtained two hysteresis loops, one for the axial loading component and another one for the shear one. Therefore, it is obtained two different hysteresis loops, which are dependent of each other. This dependence is capture by the strain amplitude ratio ($\lambda = \gamma/\varepsilon$) given by the shear strain to axial strain ratio, which is the angle in radians between the axial and shear strains amplitudes. The biaxial strain level is given by $\varepsilon_{sl} = \sqrt{\varepsilon_t^2 + \gamma_t^2}$, which is a measure that can be directly related with the strain amplitude ratio. Thus, the axial and shear hysteresis loops of a biaxial loading for a given total strain is given by Eq. (5) for the axial stress loading component, and Eq. (6) for the shear one.

$$\begin{aligned} \sigma_{right}(\varepsilon_t) &= a_{\varepsilon_t}\varepsilon_t^3 + b_{\varepsilon_t}\varepsilon_t^2 + c_{\varepsilon_t}\varepsilon_t + d_{\varepsilon_t} \\ \sigma_{left}(\varepsilon_t) &= e_{\varepsilon_t}\varepsilon_t^3 + f_{\varepsilon_t}\varepsilon_t^2 + g_{\varepsilon_t}\varepsilon_t + h_{\varepsilon_t} \end{aligned} \tag{5}$$

$$\begin{aligned}\tau_{right}(\gamma_t) &= a_{\gamma_t}\gamma_t^3 + \mathrm{b}_{\gamma_t}\gamma_t^2 + \mathrm{c}_{\gamma_t}\gamma_t + \mathrm{d}_{\gamma_t} \\ \tau_{left}(\gamma_t) &= e_{\gamma_t}\gamma_t^3 + f_{\gamma_t}\gamma_t^2 + g_{\gamma_t}\gamma_t + h_{\gamma_t}\end{aligned} \tag{6}$$

The polynomial constants of Eq. (s) (5) and (6) are obtained with a polyfit function, which has as input the output values of the P functions, please see Eq. (s) (7) to (10).

$$\left[a_{\varepsilon_t}, \mathrm{b}_{\varepsilon_t}, \mathrm{c}_{\varepsilon_t}, \mathrm{d}_{\varepsilon_t}\right] = polyfit\left(P_{axial,1}(\varepsilon_{sl},\lambda), P_{axial,2}(\varepsilon_{sl},\lambda), P_{axial,3}(\varepsilon_{sl},\lambda), P_{axial,4}(\varepsilon_{sl},\lambda)\right) \tag{7}$$

$$\left[e_{\varepsilon_t}, \mathrm{f}_{\varepsilon_t}, \mathrm{g}_{\varepsilon_t}, \mathrm{h}_{\varepsilon_t}\right] = polyfit\left(P_{axial,4}(\varepsilon_{sl},\lambda), P_{axial,5}(\varepsilon_{sl},\lambda), P_{axial,6}(\varepsilon_{sl},\lambda), P_{axial,1}(\varepsilon_{sl},\lambda)\right) \tag{8}$$

$$\left[a_{\gamma_t}, \mathrm{b}_{\gamma_t}, \mathrm{c}_{\gamma_t}, \mathrm{d}_{\gamma_t}\right] = polyfit\left(P_{shear,1}(\varepsilon_{sl},\lambda), P_{shear,2}(\varepsilon_{sl},\lambda), P_{shear,3}(\varepsilon_{sl},\lambda), P_{shear,4}(\varepsilon_{sl},\lambda)\right) \tag{9}$$

$$\left[e_{\gamma_t}, \mathrm{f}_{\gamma_t}, \mathrm{g}_{\gamma_t}, \mathrm{h}_{\gamma_t}\right] = polyfit\left(P_{shear,4}(\varepsilon_{sl},\lambda), P_{shear,5}(\varepsilon_{sl},\lambda), P_{shear,6}(\varepsilon_{sl},\lambda), P_{shear,1}(\varepsilon_{sl},\lambda)\right) \tag{10}$$

Based in experiments, the P functions have the following shape under multiaxial loading conditions, please see Eq. (s) (11) and (12).

$$P_{axial,i}(\varepsilon_{sl},\lambda) = a_i + b_i\varepsilon_{sl} + c_i\lambda + d_i\varepsilon_{sl}^2 + e_i\lambda^2 + f_i\varepsilon_{sl}\lambda + g_i\varepsilon_{sl}^3 + h_i\lambda^3 + i_i\varepsilon_{sl}\lambda^2 + j_i\varepsilon_{sl}^2\lambda \tag{11}$$

$$P_{\mathrm{shear,j}}(\varepsilon_{sl},\lambda) = a_j + b_j\varepsilon_{sl} + c_j\lambda + d_j\varepsilon_{sl}^2 + e_j\lambda^2 + f_j\varepsilon_{sl}\lambda + g_j\varepsilon_{sl}^3 + h_j\lambda^3 + i_j\varepsilon_{sl}\lambda^2 + j_j\varepsilon_{sl}^2\lambda \tag{12}$$

The constants of each P function are presented in Tables 1 and 2.

	$P_{axial,1}(\varepsilon_{sl},\lambda)$	$P_{axial,2}(\varepsilon_{sl},\lambda)$	$P_{axial,3}(\varepsilon_{sl},\lambda)$	$P_{axial,4}(\varepsilon_{sl},\lambda)$	$P_{axial,5}(\varepsilon_{sl},\lambda)$	$P_{axial,6}(\varepsilon_{sl},\lambda)$
a	-0.03408	0.003106	-0.1717	-2.35533	0.008663	0.932681
b	481.6159	-0.12443	-40.4912	523.3197	-0.07452	-8.05794
c	-0.0783	0.000192	0.163393	-1.38413	0.003737	1.102192
d	-206.819	0.23118	134.2617	-379.461	0.406281	155.8362
e	-0.00448	1.86E-05	0.005408	0.0718	-0.00021	-0.05726
f	-0.80869	0.001098	-0.38309	-3.55155	0.007819	1.267397
g	-90.706	0.433687	57.93164	100.9811	-0.13097	-119.972
h	0.000124	-4.6E-07	-0.00016	-0.00084	2.57E-06	0.000676
i	-0.07011	6.69E-05	0.025193	0.003224	-0.00016	-0.03934
j	3.931702	-0.01128	-2.8987	1.435313	0.000804	1.018756

Table 1. Polynomial constants for the P functions for multi-axial loadings - Axial component.

	$P_{\text{shear},1}(\varepsilon_{sl},\lambda)$	$P_{\text{shear},2}(\varepsilon_{sl},\lambda)$	$P_{\text{shear},3}(\varepsilon_{sl},\lambda)$	$P_{\text{shear},4}(\varepsilon_{sl},\lambda)$	$P_{\text{shear},5}(\varepsilon_{sl},\lambda)$	$P_{\text{shear},6}(\varepsilon_{sl},\lambda)$
a	2.177984	0.038377	4.57375	-25.3663	0.210432	25.51458
b	59.35201	-0.17544	-17.7933	70.0056	-0.23946	-10.164
c	-0.4713	-0.00154	-0.2192	1.262069	-0.01213	-1.59249
d	-147.976	0.374491	59.83082	-106.496	0.200226	12.43844
e	0.013494	1.92E-05	0.00359	-0.01797	0.000207	0.028779
f	2.867768	0.003991	0.417744	1.686582	0.010154	0.953978
g	86.14576	-0.141	-35.9188	40.76676	0.008696	-1.96378
h	-9.4E-05	-6.1E-08	-1.8E-05	7.46E-05	-1.1E-06	-0.00016
i	-0.01049	-5.0E-05	-0.00508	-0.00596	-6.3E-05	-0.00441
j	-1.05301	0.004585	0.349309	-0.32904	0.000738	-0.1774

Table 2. Polynomial constants for the P functions for multi-axial loadings - Shear component.

3. RESULTS AND DISCUSSION

The AZ31B-F cyclic behaviour was experimentally obtained under strain control for the 6 loading paths depicted in Figure 2. The first loading case, Case 1, is a pure axial loading and the second one, Case 2, is a pure shear loading. Loading Cases 3, 4, and 5 are proportional loadings with λ equal to 30º, 45º, and 60º, respectively. Finally, Case 6 is a non-proportional loading case, with λ equal to 45º and phase shift equal to 90º. These loading paths were also implemented in the simulations of the Jiang & Sehitoglu model and in the phenomenological approach. The strain levels used in the simulations were equal to the ones used in experiments.

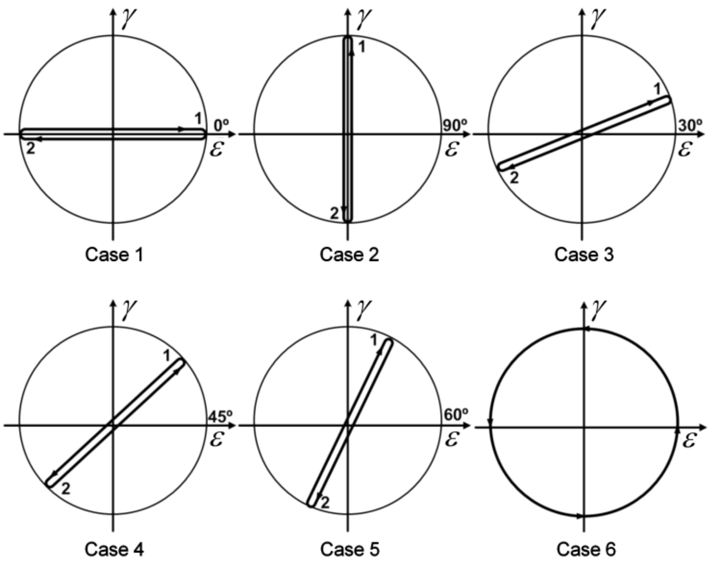

Figure 2. Biaxial loading paths: a) Case 1, b) Case 2, c) Case 3, d) Case 4, e) Case 5, and f) Case 6.

Fig. (s) 3 and 4 show the correlation between the elastic-plastic simulations and the experimental results. It was selected three strain levels in order to compare the cyclic plasticity estimates of each approach. The results correlation were presented using the stress space approach, where the axial stress vs shear stress for each strain level and loading path can be analysed. In this study, the estimates of the axial and shear stresses were not corrected by any factor as seen in the von Mises stress space, e.g. ($\sqrt{3}$).

In the experiments performed the strain time variation strictly follows the loading paths depicted in Figure 2, thus, it would be expected that the inherent stress variations should have the same loading path trajectory. However, from the experimental results it can be concluded that the result are quite different from the expected ones; much of these differences are related with the magnesium cyclic plastic behaviour. The idea here is to inspect if the simulations are able to capture this cyclic plasticity. Based in the results presented in Fig. (s) 3 and 4 it can be concluded that the phenomenological approach follows with a good accuracy the proportional loading paths obtained by experiments, only in cases 3 and 5 at 1 % of strain level it was found a slight deviation from the experimental results, please see Figure 3 e) and 4 e). The advantage of the developed phenomenological approach comparatively to the Jiang & Sehitoglu model is the possibility to simulate the effect of the λ variation in the material elastic-plastic cyclic behaviour, which has several cyclic elastic-plastic effects such as twinning and de-twinning effects. Regarding the Jiang & Sehitoglu results, it can be concluded that the estimates fail to capture the shear stress limits being higher than they should be. These results indicate that the Jiang & Sehitoglu yield function calculates higher equivalent stresses than it should in the AZ31B-F magnesium alloy, moreover the stress amplitude ratios are quite different from the experimental strain amplitude ratios. One reason that can explain these results can be found in the hardening and flow rules estimates, where the hardening rule embedded in the Jiang & Sehitoglu do not follows the magnesium hardening behaviour. This deviation from the experimental results may have some practical consequences such as the negative influence on the estimates of the crack initiation planes in magnesium alloys.

The Jiang & Sehitoglu estimates for the axial stress limits are also different from the experimental results, however, this difference is not so pronounced as is the case of shear stresses. Under proportional loadings, the Jiang & Sehitoglu estimates for tension stresses are lower than they should be, which indicates that the hardening rule do not captures the magnesium hardening in tension, however at compression the estimates are very similar to the experimental results because the magnesium hardening in compression is very low. The Jiang & Sehitoglu estimates presents symmetry in the stress space, i.e. shear and axial stresses amplitudes have the same absolute value in both loading directions. This result confirms the incapability of this constitutive model to estimate cyclic anisotropy. Figure 4 a), c), and e) presents the results for the case 5, which have a λ equal to 60º, in this loading case the shear strain amplitude is higher than the axial one. Also in this case, the Jiang & Sehitoglu model over estimates the shear stress limits, surprisingly for 1% of total strain, the axial stress estimates are very similar to the experimental ones, please see Figure 4 e). At this strain level, the phenomenological approach also have a slight deviation as can be seen in loading case 3.

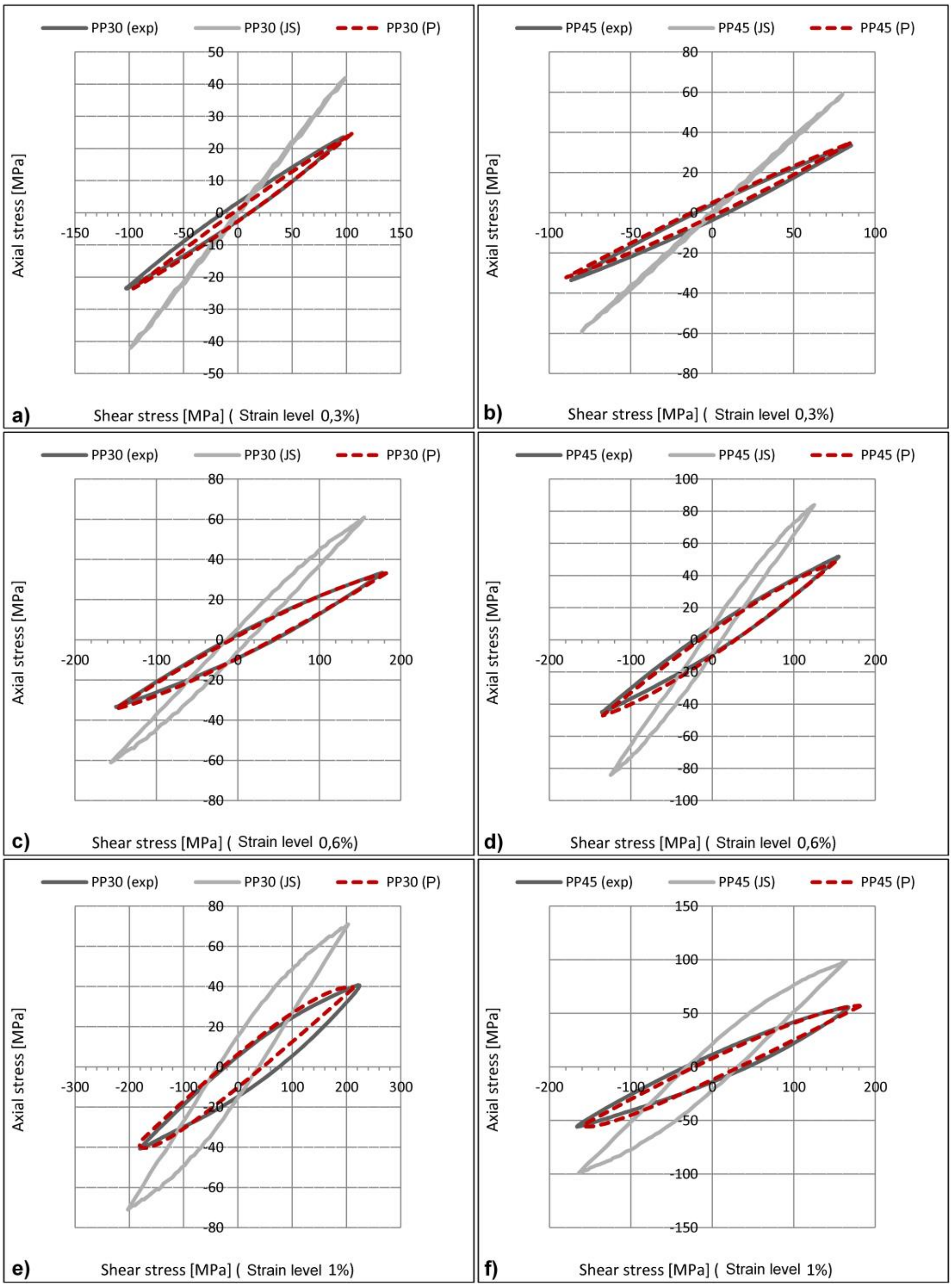

Figure 3 Correlation between estimations and experiments for loading cases (JS indicates Jiang & Sehitoglu and P indicates Phenomenological): a), c), e) Case 3, and b), d), f) Case 4.

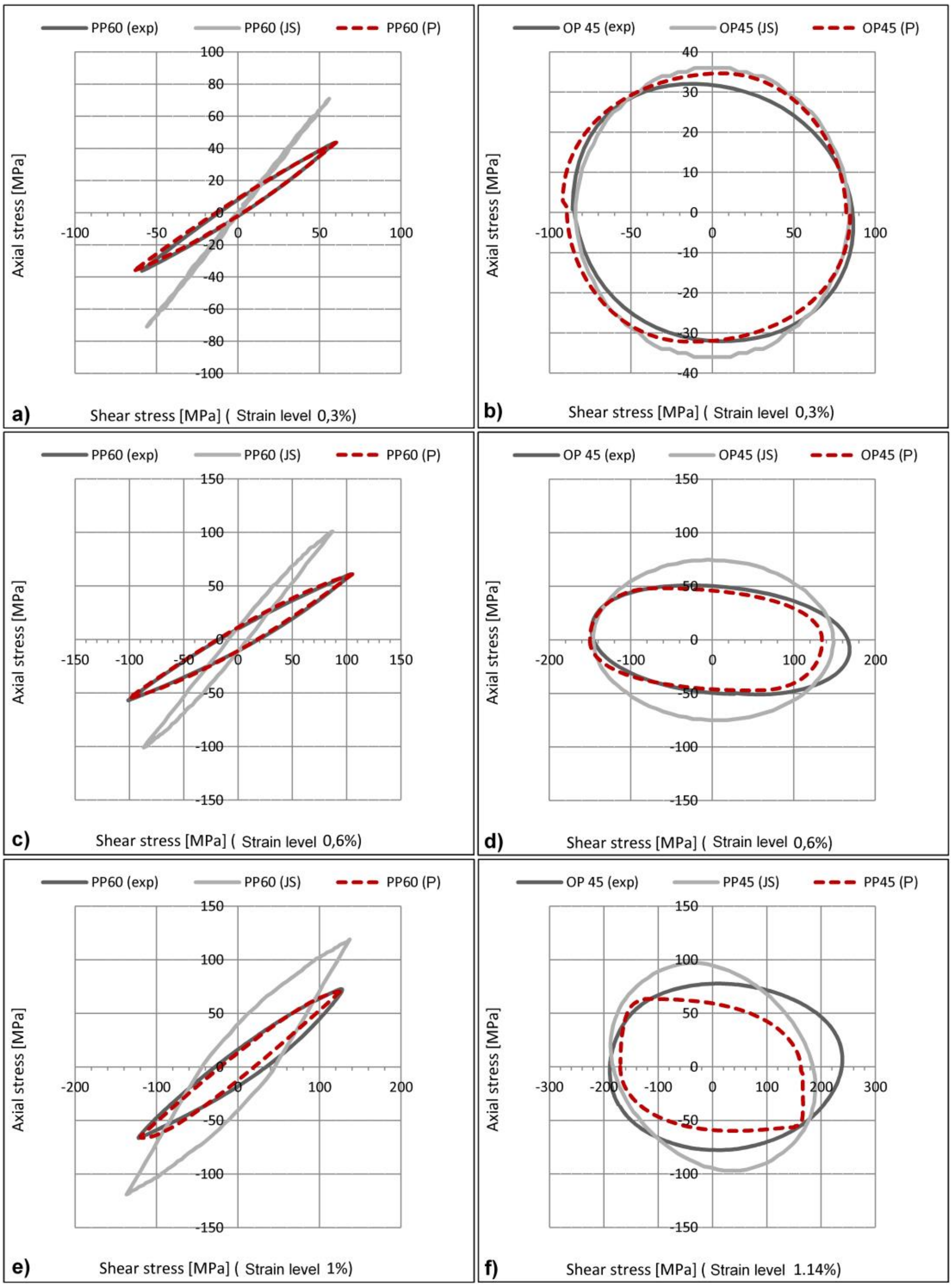

Figure 4 Correlation between estimations and experiments for loading cases (JS indicates Jiang & Sehitoglu and P indicates Phenomenological): a), c), e) Case 5, and b), d), f) Case 6.

Regarding the non-proportional results, both methods fail to follow the experimental results, only for a strain level equal to 0.3% the results were more or less acceptable, despite that, the phenomenological approach is the one that is closest to the experimental results. For instance, Figure 4 d) shows the phenomenological approach estimates, which almost fits the experimental results. The estimates fail in the tensile region where a more pronounced hardening occurs. For 1.14% of total strain, Figure 4 f), the phenomenological estimates are inside of the experimental loading path. In this case, the stress values are lower than they should be, which indicates that the phenomenological approach do not capture the non-proportional hardening behaviour of magnesium alloys, this evidence becomes more obvious with the increment of the strain level.

4. CONCLUSIONS

In this work it was studied the cyclic elastic-plastic behaviour of a magnesium alloy under multiaxial loading conditions. It were carried out several proportional and non-proportional loading paths under strain control in order to acquire the relation between the biaxial stress components as well as the plastic strains and back stresses. The idea was to analyse the λ (strain amplitude ratio) effect in the elastic-plastic parameters under proportional loadings and also analyse the non-proportional effect in those properties under a fixed λ. Experimental results were correlated with two elastic-plastic approaches, the well-known Jiang & Sehitoglu model and a phenomenological approach developed by the present authors. Results show that the experimental hysteresis loops are also asymmetric under multiaxial loading conditions, especially the ones from the axial components; the asymmetry found in the shear loading components came from the first loading direction. The Jiang & Sehitoglu model have poor estimates in proportional and non-proportional loadings, this performance can be explained by the inability to following the magnesium hardening behaviour, this conclusion was proved by the symmetry found in their estimates. The developed approach shows limitations that need to be overcome, i.e. the lack of a parameter that tunes the non-proportional hardening in combined effect. Despite this limitation, the developed approach shows good agreement with the experimental data under proportional loadings. This approach captures very well the plastic strains, and back stresses for a wide range of biaxial loading conditions.

5 ACKNOWLEDGEMENTS

The authors gratefully acknowledge financial support from FCT - Fundação para Ciência e Tecnologia (Portuguese Foundation for Science and Technology), through the project PTDC/EME-PME/104404/2008.

REFERENCES

[1] Y. Jiang, J. Zhang, "Benchmark experiments and characteristic cyclic plasticity deformation". *International Journal of Plasticity*. Vol. **24**, pp. 1481–515, (2008).

[2] JAB. Mousa, *Multiaxial Fatigue Characterization and Modeling of AZ31B Magnesium Extrusion*. University of Waterloo, (2011).

[3] H. Wang, PD. Wu, J. Wang, CN. Tomé, "A crystal plasticity model for hexagonal close packed (HCP) crystals including twinning and de-twinning mechanisms". *International Journal of Plasticity*. Vol. **49**, pp. 36–52, (2013).

[4] C. Bruni, A. Forcellese, F. Gabrielli, M. Simoncini. "Post-welding formability of AZ31 magnesium alloy". *Materials & Design.* Vol. **32**, pp.2988–91, (2011).

[5] J. Albinmousa, H. Jahed, S. Lambert, *An energy-based fatigue model for wrought magnesium alloy under multiaxial load.* ICMFF9, (2013).

[6] J. Albinmousa, H. Jahed, S. Lambert, "Cyclic axial and cyclic torsional behaviour of extruded AZ31B magnesium alloy". *International Journal of Fatigue*. Vol. **33**, pp. 1403–16, (2011).

[7] V. Anes, L. Reis, M. Freitas, "Evaluation of the AZ31 cyclic elastic-plastic behaviour under multiaxial loading conditions". *Fract. Structural Integrity*, pp. 282–92, (2014).

[8] L. Reis, V. Anes, M. de Freitas, "AZ31 magnesium alloy multiaxial LCF behavior: theory, simulation and experiments". *Advanced Materials Research*. Vol. **891**, pp. 1366–71, (2014).

[9] Y. Jiang, P. Kurath, "A theoretical evaluation of plasticity hardening algorithms for nonproportional loadings". *Acta Mechanica*. Vol. **118**, pp. 213–34, (1996).

[10] J. Koike, "Enhanced deformation mechanisms by anisotropic plasticity in polycrystalline Mg alloys at room temperature". *Metallurgical and Materials Transactions A*. Vol. **36**, 1689–96, (2005).

[11] H. Wang, B. Raeisinia, PD. Wu, SR. Agnew, CN. Tomé, "Evaluation of self-consistent polycrystal plasticity models for magnesium alloy AZ31B sheet". *International Journal of Solids and Structures*. Vol. **47**, pp. 2905–17, (2010).

[12] H. Wang, PD. Wu, J. Wang, "Modeling inelastic behavior of magnesium alloys during cyclic loading–unloading". *Internat. Journal of Plasticity*. Vol. **47**, pp. 49–64, (2013).

[13] L. Wu, A. Jain, DW. Brown, GM. Stoica, R. Agnew S, B. Clausen, "Twinning–detwinning behavior during the strain-controlled low-cycle fatigue testing of a wrought magnesium alloy, ZK60A". *Acta Materialia*. Vol. **56**, pp. 688–95, (2008).

[14] K. Chung, M-G. Lee, D. Kim, C. Kim, ML. Wenner, F. Barlat, "Spring-back evaluation of automotive sheets based on isotropic-kinematic hardening laws and non-quadratic anisotropic yield functions: Part I: theory and formulation". *International Journal of Plasticity*. Vol. 21, pp. 861–82, (2005).

[15] L. Reis, V. Anes, B. Li, M. de Freitas, "Characterizing the Cyclic Behaviour of Extruded AZ31 Magnesium Alloy". *Materials Science Forum*. Vol. **730**, pp. 727–32, (2013).

[16] V. Anes, L. Reis, B. Li, M. Fonte, M. de Freitas, "New approach for analysis of complex multiaxial loading paths". *International Journal of Fatigue*, Vol. **62**, pp. 21–33, (2014).

[17] Y. Jiang, H. Sehitoglu, "Modeling of cyclic ratchetting plasticity, part I: development of constitutive relations". *Journal of Applied Mechanics*, Vol. **63**, pp. 720–5, (1996).

[18] Y. Jiang, P. Kurath, "Nonproportional cyclic deformation: critical experiments and analytical modeling". *International Journal of Plasticity*. Vol. **13**, pp. 743–63, (1996).